

pFedES: Model Heterogeneous Personalized Federated Learning with Feature Extractor Sharing

Liping Yi^a, Han Yu^{b,*}, Gang Wang^{a,†}, Xiaoguang Liu^a

^a College of Computer Science, Nankai University, Tianjin, China

^b School of Computer Science and Engineering, Nanyang Technological University, Singapore

{yiliping, wgzwp, liuxg}@nbsj1.nankai.edu.cn, han.yu@ntu.edu.sg

Abstract

As a privacy-preserving collaborative machine learning paradigm, federated learning (FL) has attracted significant interest from academia and the industry alike. To allow each data owner (a.k.a., FL clients) to train a heterogeneous and personalized local model based on its local data distribution, system resources and requirements on model structure, the field of model-heterogeneous personalized federated learning (MHPFL) has emerged. Existing MHPFL approaches either rely on the availability of a public dataset with special characteristics to facilitate knowledge transfer, incur high computation and communication costs, or face potential model leakage risks. To address these limitations, we propose a model-heterogeneous personalized Federated learning approach based on feature Extractor Sharing (pFedES). It incorporates a small homogeneous feature extractor into each client’s heterogeneous local model. Clients train them via the proposed iterative learning method to enable the exchange of global generalized knowledge and local personalized knowledge. The small local homogeneous extractors produced after local training are uploaded to the FL server and for aggregation to facilitate easy knowledge sharing among clients. We theoretically prove that pFedES can converge over wall-to-wall time. Extensive experiments on two real-world datasets against six state-of-the-art methods demonstrate that pFedES builds the most accurate model, while incurring low communication and computation costs. Compared with the best-performing baseline, it achieves 1.61% higher test accuracy, while reducing communication and computation costs by 99.6% and 82.9%, respectively.

*Corresponding author

†Corresponding author

1. Introduction

Federated learning (FL) [11] is an emerging collaborative machine learning paradigm. It often relies on a central FL server to coordinate decentralized data owners (a.k.a., FL clients) to train a shared global FL model in a privacy-preserving manner [20]. Due to its potential to help artificial intelligence (AI) applications comply with privacy regulations, FL has been widely adopted in various fields, including computer vision (CV) [27], healthcare [28] and power generation [6]. In a traditional FL system, the server first broadcasts the global model to clients. Clients then train the received global model on their respective local dataset and upload the trained local models to the server. The server aggregates the received local models to update the global model. These steps are repeated until the global model converges. During the entire training process, only models are transmitted between the server and clients, while the data never leaves clients, thereby protecting data privacy.

The above prevailing mode of FL follows the model homogeneity assumption. It requires that all clients train local models with the same structure as the global model. Thus, it is still equipped to address the following important challenges often encountered in practice:

- **Data Heterogeneity.** Clients can own non-independently and identically distributed (non-iid) data [41]. Directly aggregating biased Local models trained on such data can lead to sub-optimal global models [52].
- **Resource Heterogeneity.** FL clients are often devices (e.g., mobile phones, autonomous vehicles) with divergent system resources in terms of computational power and communication bandwidth [19]. Low-end devices can only train small models, while high-end devices can train large models. In the face of such resource heterogeneity, the traditional FL approach is only able to limit all clients to train the smallest denomination of the model, leading to model performance bottlenecks and wasted system resources for high-end devices.
- **Model Ownership Heterogeneity.** In cases where FL

clients are companies, they often fine-tune models from their internal repositories via FL. Different companies often maintain models with distinct structures. Due to intellectual property considerations [45], they are reluctant to expose their models to others. Therefore, it is desirable to allow each FL client to train a local model following a unique structure to prevent model leakage to others.

To address the above challenges simultaneously, the field of model-heterogeneous personalized federated learning (MHPFL) has emerged. It focuses on enabling each FL client to train a personalized and heterogeneous model based on its local data distribution, system resources, and model structure requirements [46]. Prior efforts for MHPFL can be divided into three main branches: 1) knowledge distillation, 2) mutual learning, and 3) model mixup.

Knowledge distillation-based MHPFL methods either depend on a public dataset which is not always available [25], or introduce heavy communication costs [7], computation overheads [14], and risks of privacy leakage [40, 42]. *Mutual learning-based MHPFL methods* [38, 44] train a local heterogeneous large model and a homogeneous small model on clients with a mutual learning approach and share the homogeneous small models for information fusion across different clients. Since there is no discussion about the relationship between the two models in model capacity or structure, model performance is limited, with extra computational costs incurred by clients. *Model mixup-based MHPFL methods* [9, 24] split each client’s local heterogeneous model into a homogeneous part and a heterogeneous part, and only share the homogeneous parts across clients. Only part of a complete local model (partial knowledge) is being shared, which leads to model performance bottleneck and leakage of the shared model structure.

To tackle the above limitations of existing MHPFL methods, we propose an efficient model-heterogeneous personalized Federated learning framework based on small homogeneous feature Extractor Sharing (pFedES). It incorporates a small homogeneous feature extractor into each client’s local heterogeneous model. Clients train these two models following the proposed iterative learning method to facilitate the exchange of globally generalized knowledge and locally personalized knowledge. The updated homogeneous feature extractors are then uploaded to the FL server for aggregation to facilitate knowledge sharing among heterogeneous local models. Since only the small homogeneous feature extractors are transmitted between the server and clients, pFedES incurs low communication costs and protects the privacy of local data as well as local model intellectual properties. Since only one extra small homogeneous feature extractor is being trained by each client, the extra computational overhead introduced is low.

Through theoretical analysis, we show the non-convex convergence rate of pFedES and prove it converges over

wall-to-wall time. Extensive experiments on two real-world datasets against six state-of-the-art methods demonstrate that pFedES builds the most accurate model, while incurring low communication and computation costs. Compared with the best-performing baseline, it achieves 1.61% higher test accuracy, while reducing communication and computation costs by 99.6% and 82.9%, respectively.

2. Related Work

Existing MHPFL methods have two families: a) *partially model-heterogeneous*, clients hold different subnets of the global model, and heterogeneous subnets can be aggregated on the server, such as FedRolex [3], HeteroFL [10], FjORD [13], HFL [29], Fed2 [47], FedResCuE [54]. b) *fully model-heterogeneous*, clients can hold models with completely different structures. These fully heterogeneous local models cannot be aggregated directly on the server. This branch of work involves the following three categories.

Knowledge Distillation-based MHPFL. For *public dataset-dependent* knowledge distillation-based MHPFL methods (such as Cronus [4], FedGEMS [7], Fed-ET [8], FSFL [15], FCCL [14], DS-FL [16], FedMD [22], FedKT [23], FedDF [25], FedHeNN [30], FedAUX [35], CFD [36], FedKEMF [48] and KT-pFL [49]), the server aggregates the output logits of local heterogeneous models on a public dataset to construct the global logits. Clients then calculate the distance between the global logits and the local logits of their respective local heterogeneous models on the same public dataset as a distillation loss for training the local heterogeneous model. However, the public dataset is not always accessible and should have the same distribution as private data. Besides, computing and transmitting the logits for each public data sample incurs high extra computation and communication costs. Data privacy may be compromised by paired-logits inversion attacks [40].

For other knowledge distillation-based MHPFL methods *not dependent on a public dataset*, FedZKT [50] and FedGen [53] introduce zero-shot knowledge distillation to FL. They generate a public dataset by training a generator, which is time-consuming. HFD [1, 2], FedGKT [12], FD [18] and FedProto [42] allow each client to upload the (average) logits or representations of its local seen-class samples to the server. Then, the server aggregates logits or representations by classes, and the updated global class-logits or representations are sent back to clients and used to calculate the distillation loss with local logits. Clients under these methods are required to calculate distillation loss for each local data sample, incurring high computation costs. Besides, the uploaded logits or representations and the corresponding class information might compromise privacy.

Mutual Learning-based MHPFL. In FML [38] and FedKD [44], each client owns a small homogeneous model and a large heterogeneous model trained via mutual learn-

ing. The trained small homogeneous models are aggregated by the server, i.e., the small homogeneous models serve as information media to facilitate knowledge transfer among local large heterogeneous models. However, they do not explore the relationship between the two models in model structure and parameter capacity, which negatively affects the final model performance and incurs high computation costs for training an extra homogeneous model for clients.

Model Mixup-based MHPFL. These methods split each client’s local model into two parts: a feature extractor and a classifier, and only one part is shared. FedMatch [5], FedRep [9], FedBABU [32] and FedAlt/FedSim [33] share the homogeneous feature extractor to enhance model generalization while preserving the personalized local classifier. In contrast, FedClassAvg [17], LG-FedAvg [24] and CHFL [26] share the homogeneous classifier to improve model classification while preserving the personalized local feature extractor. Since only part of the entire model is shared, the final local heterogeneous models face performance bottlenecks. Besides, they are also prone to leaking the structure of the shared part of the model.

In contrast, pFedES incorporates the global information carried by the global feature extractor as prior knowledge into the local heterogeneous model to enhance its generalization. As only the additional homogeneous feature extractors are exchanged between the server and the clients for knowledge transfer, while local heterogeneous models always stay with the clients, pFedES preserves model structure privacy while facilitating collaboration among the heterogeneous models from different FL clients.

3. Preliminaries

FedAvg [31] is a typical FL algorithm. It assumes that a FL system consists of one central FL server and N FL clients. In each communication round, the server randomly selects a fraction C of N clients (the selected client set is S , $|S| = C \cdot N = K$), and broadcasts the global model $\mathcal{F}(\omega)$ ($\mathcal{F}(\cdot)$ is model structure, ω are model parameters) to them. A client k trains the received global model $\mathcal{F}(\omega)$ on its local dataset D_k ($D_k \sim P_k$, D_k obeys distribution P_k , i.e., local data from different clients are non-IID) to obtain an updated local model $\mathcal{F}(\omega_k)$ via gradient descent, i.e., $\omega_k \leftarrow \omega - \eta \nabla \ell(\mathcal{F}(\mathbf{x}_i; \omega), y_i)$. $\ell(\mathcal{F}(\mathbf{x}_i; \omega), y_i)$ is the loss of the global model $\mathcal{F}(\omega)$ on the sample $(\mathbf{x}_i, y_i) \in D_k$. The updated local model $\mathcal{F}(\omega_k)$ is uploaded to the server. The server aggregates the received local models from K clients via weighted averaging to update the global model, i.e., $\omega = \sum_{k=0}^{K-1} \frac{n_k}{n} \omega_k$ ($n_k = |D_k|$ is the data volume of client k , $n = \sum_{k=0}^{N-1} n_k$ is total data volume of all clients).

In short, the typical FL algorithm requires all clients to train local models with the same structures (**homogeneous**), and its training objective is to minimize the average loss of

the global model $\mathcal{F}(\omega)$ on all client data, i.e.,

$$\min_{\omega \in \mathbb{R}^d} \sum_{k=0}^{K-1} \frac{n_k}{n} \mathcal{L}_k(\mathcal{F}(\omega); D_k), \quad (1)$$

where the parameters of the global model, ω , are d -dimensional real numbers. $\mathcal{L}_k(\mathcal{F}(\omega); D_k)$ is the average loss of the global model $\mathcal{F}(\omega)$ on client k ’s local data D_k .

The objective of this paper is to study MHPFL in the context of supervised image classification tasks. We assume that all clients execute the same set of image classification tasks, and different clients hold heterogeneous local models with different structures, i.e., $\mathcal{F}_k(\omega_k)$ ($\mathcal{F}_k(\cdot)$ is the heterogeneous model structure, ω_k denotes personalized model parameters). pFedES aims to minimize the loss sum of all local heterogeneous personalized models, i.e.,

$$\min_{\omega_0, \dots, \omega_{K-1} \in \mathbb{R}^{d_0, \dots, d_{K-1}}} \sum_{k=0}^{K-1} \mathcal{L}_k(\mathcal{F}_k(\omega_k); D_k), \quad (2)$$

where the parameters $\omega_0, \dots, \omega_{K-1}$ of local heterogeneous models are d_0, \dots, d_{K-1} -dimensional real numbers.

4. The Proposed pFedES Approach

To achieve the above design objective, pFedES incorporates an additional small homogeneous feature extractor $\mathcal{G}(\theta_k)$ ($\mathcal{G}(\cdot)$ is the structure of the homogeneous extractor, θ_k denotes the personalized parameters of client k ’s extractor) into each FL client k . Clients then transfer knowledge across their heterogeneous local models by sharing their small homogeneous feature extractors. In training round t , pFedES performs the following steps:

1. The server selects K clients among N clients following some client selection approach [39], and broadcasts the global feature extractor $\mathcal{G}(\theta^{t-1})$ aggregated in the $(t - 1)$ -th round to the selected clients.

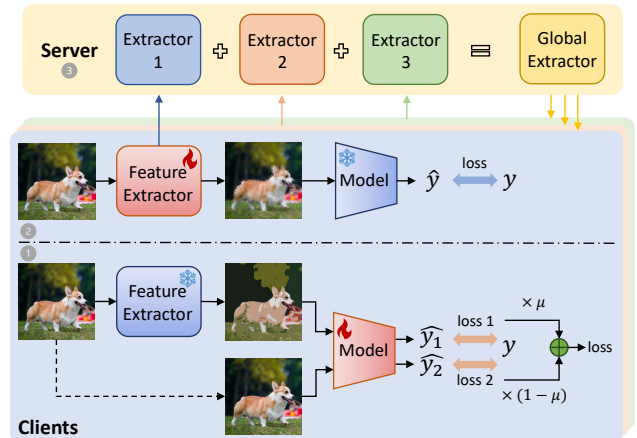


Figure 1. Workflow of pFedES.

2. Client k trains the received global feature extractor $\mathcal{G}(\theta^{t-1})$ and local model $\mathcal{F}_k(\omega_k^{t-1})$ on its local data D_k following the proposed *iterative training* method. Afterwards, the local feature extractor $\mathcal{G}(\theta_k^t)$ is uploaded to the FL server, while the heterogeneous local model $\mathcal{F}_k(\omega_k^t)$ remains within the client.
 3. The server aggregates the received client feature extractors $\mathcal{G}(\theta_k^t)$ to update the global feature extractor $\mathcal{G}(\theta^t)$.
- The above steps are repeated until all clients' heterogeneous local models converge. Finally, each client's personalized heterogeneous local model is used for inference. The details of pFedES are described in Algorithm 1.

4.1. Iterative Training

To facilitate effective global and local knowledge transfer, we design a novel iterative training method to train each client's homogeneous feature extractor and heterogeneous local model.

1. The global homogeneous feature extractor received from the server by a client is frozen. The local data are inputted as prompt information into the frozen global extractor carrying global knowledge to obtain the *enhanced data* containing both global knowledge and local personalized knowledge. Then, both the local data and the enhanced data are used to train the heterogeneous local model to achieve *global-to-local* knowledge transfer.
2. The heterogeneous local model is frozen after training in the first step. Then, the homogeneous feature extractor is trained with local data to achieve *local-to-global* knowledge transfer.

Freeze Extractor, Train Local Model Following Step ① as shown in Figure 1, in round t , for client k , freezing the global extractor $\mathcal{G}(\theta^{t-1})$ from the server and training the heterogeneous local model $\mathcal{F}_k(\omega_k^{t-1})$ includes two data inputs: 1) client k 's original local data $(\mathbf{x}, y) \in D_k$ being inputted into $\mathcal{G}(\theta^{t-1})$ to obtain the enhanced data $\hat{\mathbf{x}} = \mathcal{G}(\theta^{t-1}; \mathbf{x})$ ($\hat{\mathbf{x}}$ and \mathbf{x} are of the same dimension); 2) client k 's original local data $(\mathbf{x}, y) \in D_k$. Both data are inputted into $\mathcal{F}_k(\omega_k^{t-1})$ to produce predictions:

$$\hat{y}_1 = \mathcal{F}_k(\omega_k^{t-1}; \hat{\mathbf{x}}); \hat{y}_2 = \mathcal{F}_k(\omega_k^{t-1}; \mathbf{x}). \quad (3)$$

Then, k calculates the hard loss (e.g., cross-entropy loss [51]) between the predictions \hat{y}_1, \hat{y}_2 and the label y ,

$$\ell_1 = \ell(\hat{y}_1, y), \ell_2 = \ell(\hat{y}_2, y). \quad (4)$$

In earlier training rounds, the global extractor might be unstable. The enhanced data produced by a poor-performing global extractor might be of low quality, thereby negatively impacting the performance of the heterogeneous local model. To balance the global knowledge and the local personalized knowledge carried by the two types of input

Algorithm 1: pFedES

Input: N , total number of clients; K , number of selected clients in one round; T , total number of rounds; η_ω , learning rate of heterogeneous local models; η_θ , learning rate of local extractors; μ , weight of loss for the combination of the frozen extractor and the training heterogeneous local model.

Output: $[\mathcal{F}_0(\omega_0^{T-1}), \dots, \mathcal{F}_{N-1}(\omega_{N-1}^{T-1})]$.

Randomly initialize heterogeneous local models $[\mathcal{F}_0(\omega_0^0), \dots, \mathcal{F}_k(\omega_k^0), \dots, \mathcal{F}_{N-1}(\omega_{N-1}^0)]$ and the global extractor $\mathcal{G}(\theta^0)$.

for each round $t=1, \dots, T-1$ **do**

 // **Server Side:**

$S^t \leftarrow$ Randomly sample K clients from N clients;

 Broadcast the global extractor θ^{t-1} to K clients;

$\theta_k^t \leftarrow$ **ClientUpdate**(θ^{t-1});

 /* Aggregate Local Extractor */

$$\theta^t = \sum_{k=0}^{K-1} \frac{n_k}{n} \theta_k^t.$$

 // **ClientUpdate:**

 Receive the global extractor θ^{t-1} from the server;

for $k \in S^t$ **do**

 /* Local Iterative Training */

 // Freeze Extractor, Train Model

for $(\mathbf{x}, y) \in D_k$ **do**

$$\hat{\mathbf{x}} = \mathcal{G}(\theta^{t-1}; \mathbf{x});$$

$$\hat{y}_1 = \mathcal{F}_k(\omega_k^{t-1}; \hat{\mathbf{x}}); \hat{y}_2 = \mathcal{F}_k(\omega_k^{t-1}; \mathbf{x});$$

$$\ell_1 = \ell(\hat{y}_1, y), \ell_2 = \ell(\hat{y}_2, y);$$

$$\ell_\omega = \mu \cdot \ell_1 + (1 - \mu) \cdot \ell_2;$$

$$\omega_k^t \leftarrow \omega_k^{t-1} - \eta_\omega \nabla \ell_\omega;$$

end

 // Freeze Model, Train Extractor

for $(\mathbf{x}, y) \in D_k$ **do**

$$\hat{\mathbf{x}} = \mathcal{G}(\theta^{t-1}; \mathbf{x});$$

$$\hat{y} = \mathcal{F}_k(\omega_k^t; \hat{\mathbf{x}});$$

$$\ell_\theta = \ell(\hat{y}, y);$$

$$\theta_k^t \leftarrow \theta^{t-1} - \eta_\theta \nabla \ell_\theta;$$

end

 Upload updated local extractor θ_k^t to the server.

end

end

Return heterogeneous personalized local models

$$[\mathcal{F}_0(\omega_0^{T-1}), \mathcal{F}_1(\omega_1^{T-1}), \dots, \mathcal{F}_k(\omega_k^{T-1}), \dots, \mathcal{F}_{N-1}(\omega_{N-1}^{T-1})].$$

data, we compute a weighted sum of the hard loss of the two data inputs as the complete loss of the heterogeneous local model:

$$\ell_\omega = \mu \cdot \ell_1 + (1 - \mu) \cdot \ell_2, \mu \in (0, 0.5]. \quad (5)$$

With the complete loss, the parameters of the heterogeneous local model are updated via gradient descent (e.g., SGD [34]):

$$\omega_k^t \leftarrow \omega_k^{t-1} - \eta_\omega \nabla \ell_\omega. \quad (6)$$

η_ω is the learning rate of the heterogeneous local model.

During this step of training, the global knowledge from the frozen global extractor is transferred to the heterogeneous local model through the enhanced data, thereby improving its generalization. The local personalized knowledge in the original local data is further incorporated into the heterogeneous local model, thereby enhancing its personalization.

Freeze Local Model, Train Extractor Following Step ② as shown in Figure 1, the heterogeneous local model $\mathcal{F}_k(\omega_k^t)$ trained in Step ① is frozen and the global feature extractor $\mathcal{G}(\theta^{t-1})$ is trained. Client k inputs its local data $(x, y) \in D_k$ into $\mathcal{G}(\theta^{t-1})$ to generate the enhanced data $\hat{x} = \mathcal{G}(\theta^{t-1}; x)$. Then, it inputs \hat{x} into the frozen $\mathcal{F}_k(\omega_k^t)$ to obtain:

$$\hat{y} = \mathcal{F}_k(\omega_k^t; \hat{x}). \quad (7)$$

Then, k computes the hard loss between the prediction \hat{y} and label y as:

$$\ell_\theta = \ell(\hat{y}, y). \quad (8)$$

After obtaining the loss, k updates the parameters of the feature extractor via gradient descent:

$$\theta_k^t \leftarrow \theta^{t-1} - \eta_\theta \nabla \ell_\theta. \quad (9)$$

η_θ is the learning rate of the feature extractor. During this step, personalized local knowledge is transferred into the updated homogeneous local feature extractor, which in turn, is uploaded to the FL server for aggregation.

4.2. Homogeneous Extractor Aggregation

After receiving the local feature extractors $\mathcal{G}(\theta_k^t)$ from selected clients, the server aggregates them following FedAvg to facilitate knowledge fusion across clients:

$$\theta^t = \sum_{k=0}^{K-1} \frac{n_k}{n} \theta_k^t. \quad (10)$$

4.3. Feature Extractor Structure

Since FL clients often are mobile edge devices with limited computational power, pFedES must improve the performance of local heterogeneous locals without introducing too much computation costs. Therefore, we design a small CNN model consisting of two convolutional layers with ‘padding=same’ as the feature extractor, as shown in Figure 2. Setting ‘padding=same’ is to guarantee the dimensions of the original data input into the feature extractor and the enhanced data output by the feature extractor are the same. We use this small CNN as the default feature extractor in subsequent experiments.

4.4. Discussion

Here, we discuss pFedES’s computational costs, communication overheads and privacy preservation.

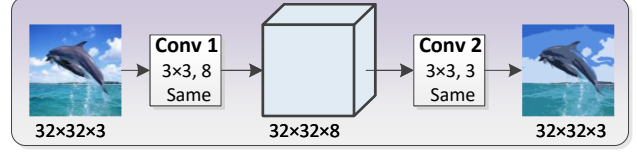


Figure 2. The structure of the homogeneous extractor in pFedES.

Computational Cost. On top of training heterogeneous local models, clients also train an additional small homogeneous feature extractor. Since we design a small CNN with two convolutional layers as the feature extractor, training it introduces low computational costs.

Communication Overhead. Since only the small homogeneous feature extractors are transmitted between the server and the clients, pFedES incurs much lower communication overhead than transmitting the complete models as in FedAvg.

Privacy Preservation. Since only the parameters of the homogeneous feature extractors are transmitted between the server and the clients while local data and local models never leave the clients, pFedES preserves data privacy and model intellectual property.

5. Analysis

Before analyzing the convergence of pFedES, we first declare some additional notations. We use t to denote a communication round and $e \in \{0, 1, \dots, E\}$ to denote the epochs/iterations of local training. In each round, each client executes E local training iterations. $tE + e$ is the e -th iteration in the $(t + 1)$ -th round. $tE + 0$ indicates that in the $(t + 1)$ -th round, before local model training, clients receive the global extractor $\mathcal{G}(\theta^t)$ aggregated in the t -th round. $tE + E$ is the last iteration of local training, indicating the end of local training in the $(t + 1)$ -th round. We denote the combination of the frozen homogeneous feature extractor with $\mathcal{G}(\theta)$, and the training of the heterogeneous local model $\mathcal{F}_k(\omega_k)$ at the first branch of Step 1 during the iterative training process as $\mathcal{H}_k(\varphi_k) = \mathcal{G}(\theta) \circ \mathcal{F}_k(\omega_k)$. We also assume that $\mathcal{F}_k(\omega_k)$ and the combined model $\mathcal{H}_k(\varphi_k)$ use the same learning rate $\eta = \eta_\omega = \eta_\varphi$.

Assumption 1. Lipschitz Smoothness. The gradients of Client k ’s heterogeneous local model are L_1 -Lipschitz smooth, i.e.,

$$\|\nabla \mathcal{L}_k^{t_1}(\omega_k^{t_1}; x, y) - \nabla \mathcal{L}_k^{t_2}(\omega_k^{t_2}; x, y)\| \leq L_1 \|\omega_k^{t_1} - \omega_k^{t_2}\|, \quad (11)$$

$$\forall t_1, t_2 > 0, k \in \{0, 1, \dots, N - 1\}, (x, y) \in D_k.$$

The above formulation can be expressed as:

$$\mathcal{L}_k^{t_1} - \mathcal{L}_k^{t_2} \leq \langle \nabla \mathcal{L}_k^{t_2}, (\omega_k^{t_1} - \omega_k^{t_2}) \rangle + \frac{L_1}{2} \|\omega_k^{t_1} - \omega_k^{t_2}\|_2^2. \quad (12)$$

Assumption 2. Unbiased Gradient and Bounded Variance. The random gradient $g_{\omega, k}^t = \nabla \mathcal{L}_k^t(\omega_k^t; \mathcal{B}_k^t)$ (\mathcal{B} is

a batch of local data) of each client’s heterogeneous local model $\mathcal{F}_k(\omega_k)$ is unbiased, and the random gradient $g_{\varphi,k}^t = \nabla \mathcal{L}_k^t(\varphi_k^t; \mathcal{B}_k^t)$ of each client’s combined model $\mathcal{H}_k(\varphi_k)$ is also unbiased, i.e.,

$$\begin{aligned} \mathbb{E}_{\mathcal{B}_k^t \subseteq D_k} [g_{\omega,k}^t] &= \nabla \mathcal{L}_k^t(\omega_k^t), \\ \mathbb{E}_{\mathcal{B}_k^t \subseteq D_k} [g_{\varphi,k}^t] &= \nabla \mathcal{L}_k^t(\varphi_k^t), \end{aligned} \quad (13)$$

and the variance of random gradient $g_{\omega,k}^t$ and $g_{\varphi,k}^t$ is bounded by:

$$\begin{aligned} \mathbb{E}_{\mathcal{B}_k^t \subseteq D_k} [\|\nabla \mathcal{L}_k^t(\omega_k^t; \mathcal{B}_k^t) - \nabla \mathcal{L}_k^t(\omega_k^t)\|_2^2] &\leq \sigma^2, \\ \mathbb{E}_{\mathcal{B}_k^t \subseteq D_k} [\|\nabla \mathcal{L}_k^t(\varphi_k^t; \mathcal{B}_k^t) - \nabla \mathcal{L}_k^t(\varphi_k^t)\|_2^2] &\leq \delta^2. \end{aligned} \quad (14)$$

With these assumptions, we derive the following lemma and theorem (proofs can be found in Appendices 8 and 9).

Lemma 1. *Based on Assumptions 1 and 2, during local iterations $\{0, 1, \dots, E\}$ in the $(t + 1)$ -th FL training round, the loss of an arbitrary client’s heterogeneous local model is bounded by:*

$$\begin{aligned} \mathbb{E}[\mathcal{L}_{(t+1)E}] &\leq \mathcal{L}_{tE+0} + \left(\frac{L_1 \eta^2 \tilde{\mu}^2}{2} - \eta \tilde{\mu}\right) \sum_{e=0}^{E-1} \|\nabla \mathcal{L}_{tE+e}\|_2^2 \\ &\quad + \frac{L_1 \eta^2 (\sigma^2 + \delta^2)}{2}. \end{aligned} \quad (15)$$

where $\tilde{\mu} = 1 - \mu$, $\mu \in (0, 0.5]$, $\tilde{\mu} \in [0.5, 1)$.

Theorem 1. Non-convex convergence rate of pFedES. *Based on the above assumptions and lemma, for an arbitrary client and any $\epsilon > 0$, the following inequality holds:*

$$\begin{aligned} \frac{1}{T} \sum_{t=0}^{T-1} \sum_{e=0}^{E-1} \|\nabla \mathcal{L}_{tE+e}\|_2^2 &\leq \frac{\frac{1}{T} \sum_{t=0}^{T-1} (\mathcal{L}_{tE+0} - \mathbb{E}[\mathcal{L}_{(t+1)E}])}{\eta \tilde{\mu} - \frac{L_1 \eta^2 \tilde{\mu}^2}{2}} \\ &\quad + \frac{\frac{L_1 \eta^2 (\sigma^2 + \delta^2)}{2}}{\eta \tilde{\mu} - \frac{L_1 \eta^2 \tilde{\mu}^2}{2}} < \epsilon, \\ s.t. \eta &< \frac{2\epsilon \tilde{\mu}}{L_1 (\sigma^2 + \delta^2 + \tilde{\mu}^2 \epsilon)}. \end{aligned} \quad (16)$$

Hence, under pFedES, a client’s heterogeneous local model converges at a non-convex rate of $\epsilon \sim \mathcal{O}(\frac{1}{T})$.

6. Experimental Evaluation

To evaluate the performance of pFedES, we compared it against 6 state-of-the-art MHPFL approaches on 2 real-world datasets. The experiments are conducted with Pytorch on 4 NVIDIA GeForce RTX 3090 GPUs with 24G memory.¹

6.1. Experiment Setup

Datasets. We evaluate pFedES and baselines on two image classification datasets: CIFAR-10 and CIFAR-100² [21]. They are divided into non-IID datasets following the

¹Link to code omitted for double-blind review.

²<https://www.cs.toronto.edu/~7Ekriz/cifar.html>

Layer Name	CNN-1	CNN-2	CNN-3	CNN-4	CNN-5
Conv1	5×5, 16	5×5, 16	5×5, 16	5×5, 16	5×5, 16
Maxpool1	2×2	2×2	2×2	2×2	2×2
Conv2	5×5, 32	5×5, 16	5×5, 32	5×5, 32	5×5, 32
Maxpool2	2×2	2×2	2×2	2×2	2×2
FC1	2000	2000	1000	800	500
FC2	500	500	500	500	500
FC3	10/100	10/100	10/100	10/100	10/100
model size	10.00 MB	6.92 MB	5.04 MB	3.81 MB	2.55 MB

Table 1. Structures of 5 heterogeneous CNN models with convolutional layers having 5×5 kernel size and 16 or 32 filters.

method specified in [37] to facilitate MHPFL experimentation. For CIFAR-10, we assign only data from 2 out of the 10 classes to each client (non-IID: 2/10). For CIFAR-100, we assign only data from 10 out of the 100 classes to each client (non-IID: 10/100). Then, each client’s local data are further divided into the training set, the validation set, and the test set following the ratio of 8:1:1. The test set is stored by each client and follows the same distribution as the local training set.

Models. As shown in Table 1, each client trains a CNN model with output layer (i.e., the last fully connected layer) dimensions of 10 and 100 for CIFAR-10 and CIFAR-100, respectively. In model-homogeneous settings, each client has the same CNN-1 model structure. In model-heterogeneous settings, clients are randomly assigned with $\{\text{CNN-1}, \dots, \text{CNN-5}\}$ with uniform probability. For both model-homogeneous and model-heterogeneous settings, the structure of the homogeneous feature extractor is as shown in Figure 2.

Baselines. We compare pFedES with 6 baselines.

- Standalone, clients train local models independently;
- Public-data independent knowledge distillation-based MHPFL methods: FD [18] and FedProto [42];
- Mutual learning-based MHPFL methods FML [38] and FedKD [44];
- Model mixup-based MHPFL methods LG-FedAvg [24].

Evaluation Metrics. **1) Accuracy:** we measure the *individual test accuracy* of each client’s heterogeneous local model and calculate the *average test accuracy* of all clients’ local models. **2) Communication Cost:** We trace the number of transmitted parameters when the average model accuracy reaches the target. **3) Computation Cost:** We track the computation FLOPs consumed when the average model accuracy reaches the target.

Training Strategy. We tune the optimal FL settings for all methods via grid search. The epochs of local model training $E \in \{1, 10\}$ and the batch size of local training $B \in \{64, 128, 256, 512\}$. The optimizer for local training is SGD with learning rate $\eta = \eta_\omega = \eta_\theta = 0.01$. We also tune special hyperparameters for the baselines and report the optimal results. We adjust two hyperparameters (μ and E_{fe} , the loss weight and training epoch of the feature extractor) for pFedES to achieve the best performance. The detailed results of hyperparameter sensitivity tests are described in

Method	N=10, C=100%		N=50, C=20%		N=100, C=10%	
	CIFAR-10	CIFAR-100	CIFAR-10	CIFAR-100	CIFAR-10	CIFAR-100
Standalone	96.35	74.32	95.25	62.38	92.58	54.93
FML [38]	94.83	70.02	93.18	57.56	87.93	46.20
FedKD [44]	94.77	70.04	92.93	57.56	90.23	50.99
LG-FedAvg [24]	96.47	73.43	94.20	61.77	90.25	46.64
FD [18]	96.30	-	-	-	-	-
FedProto [42]	95.83	72.79	95.10	62.55	91.19	54.01
pFedES	96.68	74.42	95.74	63.55	92.89	55.15

Table 2. Average accuracy (%) for *model-homogeneous* scenarios. N is the total number of clients. C is the fraction of participating clients in each round. ‘-’ denotes failure to converge.

Method	N=10, C=100%		N=50, C=20%		N=100, C=10%	
	CIFAR-10	CIFAR-100	CIFAR-10	CIFAR-100	CIFAR-10	CIFAR-100
Standalone	96.53	72.53	95.14	62.71	91.97	53.04
FML [38]	30.48	16.84	-	21.96	-	15.21
FedKD [44]	80.20	53.23	77.37	44.27	73.21	37.21
LG-FedAvg [24]	96.30	72.20	94.83	60.95	91.27	45.83
FD [18]	96.21	-	-	-	-	-
FedProto [42]	96.51	72.59	95.48	62.69	92.49	53.67
pFedES	96.70	73.89	95.79	64.32	92.72	54.40

Table 3. Average accuracy for *model-heterogeneous* scenarios.

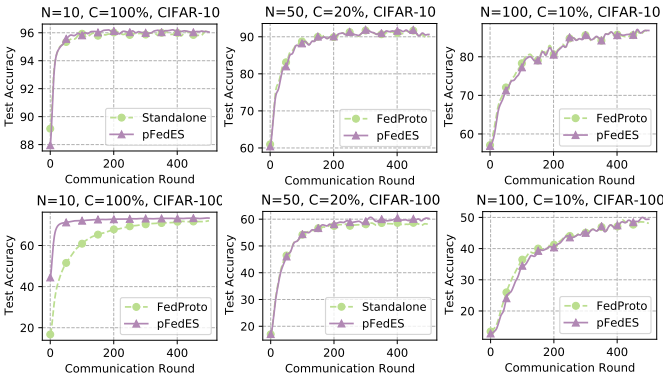


Figure 3. Average accuracy vs. communication rounds.

Appendix. 10. To compare with the baselines fairly, we set the total number of rounds $T \in \{100, 500\}$ to ensure that all algorithms converge.

6.2. Comparisons Results

We compare pFedES with baselines under both model-homogeneous and model-heterogeneous scenarios with different N and C settings. We set up three scenarios: $\{(N = 10, C = 100\%), (N = 50, C = 20\%), (N = 100, C = 10\%)\}$. For ease of comparison across the three settings, $N \times C$ is set to be the same (i.e., 10 clients participate in each round of FL). For FML and FedKD, under model-heterogeneous settings, we adopt the smallest ‘CNN-5’ model as the small homogeneous model.

Average Accuracy. The results in Tables 2 and 3 show that the average accuracy of all personalized heterogeneous local models in pFedES surpasses other baselines under both model-homogeneous and model-heterogeneous settings, by up to 1.00% and 1.61%, respectively. Figure 3 shows that pFedES converges to a higher average accuracy with faster convergence rates.

Individual Accuracy. We use box plots to display the distribution of individual model accuracy in model-heterogeneous settings. As shown in Figure 4, ‘+’ denotes

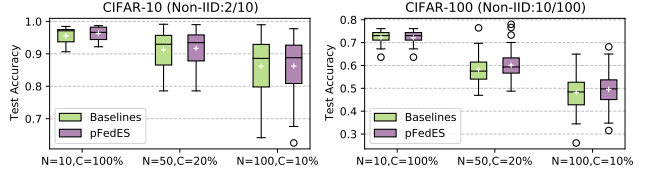


Figure 4. Accuracy distribution for individual clients.

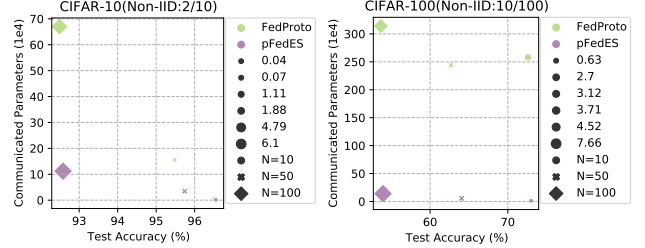


Figure 5. Trade-off among test accuracy, computational overhead and communication cost. The size of a marker reflects the computation FLOPs ($1e9$).

the average accuracy of all clients for each algorithm. A small box length bounded by the upper quartile and the lower quartile indicates a more concentrated accuracy distribution across all clients with small variance. We observe that pFedES obtains a higher average accuracy and a lower variance than the optimal baselines (Standalone or FedProto in Table 3) under most settings.

Trade-off among Accuracy, Computation & Communication Costs. We compare pFedES and the state-of-the-art baseline FedProto in terms of model accuracy, computational costs and communication costs. The target accuracy set for $N = \{10, 50, 100\}$ on CIFAR-10 dataset is 90% and that set for $N = \{10, 50, 100\}$ on CIFAR-100 dataset are $\{70\%, 60\%, 50\%\}$. As shown in Figure 5, pFedES consistently achieves the highest model accuracy with far lower communication costs than FedProto, while incurring similar computation costs. This indicates that pFedES strikes the best trade-off among the three metrics. Compared with FedProto, pFedES incurs only $\frac{1}{224}$ communication and $\frac{1}{5.85}$ computational costs (i.e., 99.6% communication and 82.9% computational cost savings), due to its faster convergence and lower per-round costs.

Visualizing Personalization. In model-heterogeneous settings, we extract every sample representation from each FL client under pFedES and FedProto. Then, we leverage T -SNE [43] to reduce the dimensionality of the extracted representations from 500 to 2, and visualize the results. Since CIFAR-100 includes 100 classes of samples, we focus on visualizing the results on CIFAR-10 (non-IID: 2/10) with $N = 10$ in Figure 6. We observe that most clusters under the two methods consist of representations from a client’s two seen classes of samples, indicating that each client’s heterogeneous local model has strong *personalization* capability. The two seen class representations within most clusters under the two methods satisfy ‘intra-class compactness

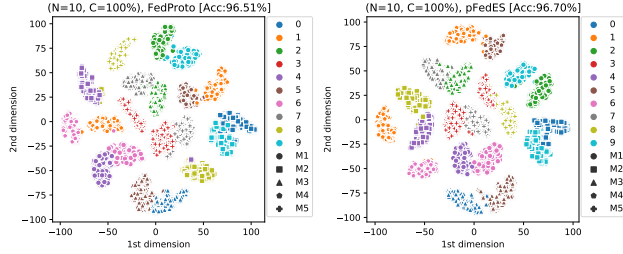


Figure 6. T-SNE representation visualization for FedProto and pFedES on CIFAR-10 (Non-IID: 2/10).



Figure 7. Visualization of original data and enhanced data.

and inter-class separation”, reflecting that every client can classify its seen classes well. Generally, pFedES achieves better classification boundaries than FedProto.

Visualizing Enhanced Data. We store the final global feature extractor trained on CIFAR-10 under the model-heterogeneous FL scenario with $N = 100$. We sample 5 original images randomly from CIFAR-10 and input them into the final global feature extractor to generate the corresponding enhanced data. The two lines in Figure 7 present the visualized results of the original data and the generated enhanced data. It can be observed that enhanced images embedded with global information still retain partial features of original images, indicating that the shared homogeneous feature extractor learns global and local personalized knowledge effectively. Besides, valid enhanced data increase the number of training samples, thereby boosting the accuracy of heterogeneous local models.

6.3. Case Studies

6.3.1 Robustness to Non-IID Data

We evaluate the robustness of pFedES and FedProto under different non-IID data settings with ($N = 100, C = 10\%$). We vary the number of classes seen by each client as $\{2, 4, 6, 8, 10\}$ on CIFAR-10 and $\{10, 30, 50, 70, 90, 100\}$ on CIFAR-100. Figure 8 shows that pFedES consistently outperforms FedProto, demonstrating its robustness to non-IID data. As the non-IID degree decreases (i.e., the number of classes seen by each client increases), the accuracy drops since more IID data enhances generalization and reduces personalization.

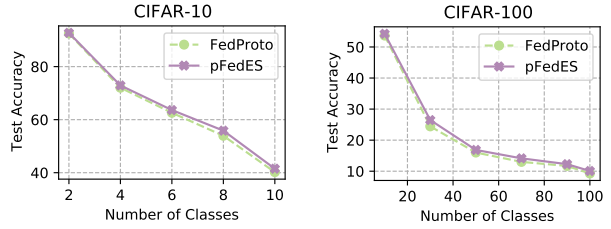


Figure 8. Robustness to Non-IID data.

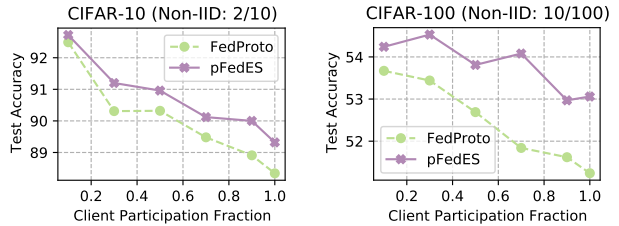


Figure 9. Robustness to client participation rates.

6.3.2 Robustness to Client Participant Rates

We also test the robustness of pFedES and FedProto against different client participant rates C under ($N = 100$) on CIFAR-10 (non-IID: 2/10) and CIFAR-100 (non-IID: 10/100). We vary the client participant rates as $C = \{0.1, 0.3, 0.5, 0.7, 0.9, 1\}$. Figure 9 shows that pFedES consistently outperforms FedProto, especially on more complicated CIFAR-100, verifying its robustness to changes in client participant rates. Besides, as the client participant rates increase, model accuracy drops as more participating clients provide more IID local data, which also improves generalization and reduces personalization.

7. Conclusions and Future Work

In this paper, we proposed a novel MHPFL approach, pFedES, based on sharing homogeneous feature extractors with efficient privacy preservation, and communication and computation cost savings. It enables each client to iteratively train a homogeneous feature extractor and heterogeneous local model to exchange global and local knowledge. Aggregating the homogeneous local feature extractors from clients fuses knowledge across their heterogeneous local models. Theoretical analysis proves its convergence. Extensive experiments demonstrate that pFedES obtains the highest model accuracy, while incurring the lowest communication and computation costs.

In subsequent research, we plan to extend pFedES in two ways: 1) exploring more efficient structures for the homogeneous feature extractor; and 2) optimizing the pattern of training the homogeneous feature extractor and the local heterogeneous model, in order to further improve model performance and reduce the additional computational costs incurred by training the homogeneous feature extractors.

References

- [1] Jin-Hyun Ahn et al. Wireless federated distillation for distributed edge learning with heterogeneous data. In *Proc. PIMRC*, pages 1–6, Istanbul, Turkey, 2019. IEEE. 2
- [2] Jin-Hyun Ahn et al. Cooperative learning VIA federated distillation OVER fading channels. In *Proc. ICASSP*, pages 8856–8860, Barcelona, Spain, 2020. IEEE. 2
- [3] Samiul Alam et al. Fedrolex: Model-heterogeneous federated learning with rolling sub-model extraction. In *Proc. NeurIPS*, virtual, 2022. . 2
- [4] Hongyan Chang et al. Cronus: Robust and heterogeneous collaborative learning with black-box knowledge transfer. In *Proc. NeurIPS Workshop*, virtual, 2021. . 2
- [5] Jiangui Chen et al. Fedmatch: Federated learning over heterogeneous question answering data. In *Proc. CIKM*, pages 181–190, virtual, 2021. ACM. 3
- [6] Yuanyuan Chen, Zichen Chen, Sheng Guo, Yansong Zhao, Zelei Liu, Pengcheng Wu, Chengyi Yang, Zengxiang Li, and Han Yu. Efficient training of large-scale industrial fault diagnostic models through federated opportunistic block dropout. In *IAAI*, pages 15485–15493, 2023. 1
- [7] Sijie Cheng et al. Fedgems: Federated learning of larger server models via selective knowledge fusion. *CoRR*, abs/2110.11027, 2021. 2
- [8] Yae Jee Cho et al. Heterogeneous ensemble knowledge transfer for training large models in federated learning. In *Proc. IJCAI*, pages 2881–2887, virtual, 2022. ijcai.org. 2
- [9] Liam Collins et al. Exploiting shared representations for personalized federated learning. In *Proc. ICML*, pages 2089–2099, virtual, 2021. PMLR. 2, 3
- [10] Enmao Diao. Heteroffl: Computation and communication efficient federated learning for heterogeneous clients. In *Proc. ICLR*, page 1, Austria, 2021. OpenReview.net. 2
- [11] Randy Goebel, Han Yu, Boi Faltings, Lixin Fan, and Zhiwei Xiong. *Trustworthy Federated Learning*. Springer, Cham, 2023. 1
- [12] Chaoyang He et al. Group knowledge transfer: Federated learning of large cnns at the edge. In *Proc. NeurIPS*, virtual, 2020. . 2
- [13] S. Horváth. FjORD: Fair and accurate federated learning under heterogeneous targets with ordered dropout. In *Proc. NIPS*, pages 12876–12889, Virtual, 2021. OpenReview.net. 2
- [14] Wenke Huang et al. Learn from others and be yourself in heterogeneous federated learning. In *Proc. CVPR*, pages 10133–10143, virtual, 2022. IEEE. 2
- [15] Wenke Huang et al. Few-shot model agnostic federated learning. In *Proc. MM*, pages 7309–7316, Lisboa, Portugal, 2022. ACM. 2
- [16] Sohei Itahara et al. Distillation-based semi-supervised federated learning for communication-efficient collaborative training with non-iid private data. *IEEE Trans. Mob. Comput.*, 22(1):191–205, 2023. 2
- [17] Jaehee Jang et al. Fedclassavg: Local representation learning for personalized federated learning on heterogeneous neural networks. In *Proc. ICPP*, pages 76:1–76:10, virtual, 2022. ACM. 3
- [18] Eunjeong Jeong et al. Communication-efficient on-device machine learning: Federated distillation and augmentation under non-iid private data. In *Proc. NeurIPS Workshop on Machine Learning on the Phone and other Consumer Devices*, virtual, 2018. . 2, 6, 7
- [19] Yuang Jiang et al. Model pruning enables efficient federated learning on edge devices. *TNNLS*, 1(1):1, 2022. 1
- [20] Peter Kairouz et al. Advances and open problems in federated learning. *Foundations and Trends in Machine Learning*, 14(1–2):1–210, 2021. 1
- [21] Alex Krizhevsky et al. *Learning multiple layers of features from tiny images*. Toronto, ON, Canada, , 2009. 6
- [22] Daliang Li and Junpu Wang. Fedmd: Heterogeneous federated learning via model distillation. In *Proc. NeurIPS Workshop*, virtual, 2019. . 2
- [23] Qinbin Li et al. Practical one-shot federated learning for cross-silo setting. In *Proc. IJCAI*, pages 1484–1490, virtual, 2021. ijcai.org. 2
- [24] Paul Pu Liang et al. Think locally, act globally: Federated learning with local and global representations. *arXiv preprint arXiv:2001.01523*, 1(1), 2020. 2, 3, 6, 7
- [25] Tao Lin et al. Ensemble distillation for robust model fusion in federated learning. In *Proc. NeurIPS*, virtual, 2020. . 2
- [26] Chang Liu et al. Completely heterogeneous federated learning. *CoRR*, abs/2210.15865, 2022. 3
- [27] Yang Liu, Anbu Huang, Yun Luo, He Huang, Youzhi Liu, Yuanyuan Chen, Lican Feng, Tianjian Chen, Han Yu, and Qiang Yang. Fedvision: An online visual object detection platform powered by federated learning. In *IAAI*, pages 13172–13179, 2020. 1
- [28] Zelei Liu, Yuanyuan Chen, Yansong Zhao, Han Yu, Yang Liu, Renyi Bao, Jinpeng Jiang, Zaiqing Nie, Qian Xu, and Qiang Yang. Contribution-aware federated learning for smart healthcare. In *IAAI*, pages 12396–12404, 2022. 1
- [29] Xiaofeng Lu et al. Heterogeneous model fusion federated learning mechanism based on model mapping. *IEEE Internet Things J.*, 9(8):6058–6068, 2022. 2
- [30] Disha Makhija et al. Architecture agnostic federated learning for neural networks. In *Proc. ICML*, pages 14860–14870, virtual, 2022. PMLR. 2
- [31] Brendan McMahan et al. Communication-efficient learning of deep networks from decentralized data. In *Proc. AISTATS*, pages 1273–1282, USA, 2017. PMLR. 3
- [32] Jaehoon Oh et al. Fedbabu: Toward enhanced representation for federated image classification. In *Proc. ICLR*, virtual, 2022. OpenReview.net. 3
- [33] Krishna Pillutla et al. Federated learning with partial model personalization. In *Proc. ICML*, pages 17716–17758, virtual, 2022. PMLR. 3
- [34] Sebastian Ruder. An overview of gradient descent optimization algorithms. *CoRR*, abs/1609.04747:1, 2016. 4
- [35] Felix Sattler et al. Fedaux: Leveraging unlabeled auxiliary data in federated learning. *IEEE Trans. Neural Networks Learn. Syst.*, 1(1):1–13, 2021. 2
- [36] Felix Sattler et al. CFD: communication-efficient federated distillation via soft-label quantization and delta coding. *IEEE Trans. Netw. Sci. Eng.*, 9(4):2025–2038, 2022. 2

- [37] Aviv Shamsian et al. Personalized federated learning using hypernetworks. In *Proc. ICML*, pages 9489–9502, virtual, 2021. PMLR. [6](#)
- [38] Tao Shen et al. Federated mutual learning. *CoRR*, abs/2006.16765, 2020. [2](#), [6](#), [7](#)
- [39] Yuxin Shi, Han Yu, and Cyril Leung. Towards fairness-aware federated learning. *IEEE Transactions on Neural Networks and Learning Systems*, 2023. [3](#)
- [40] Hideaki Takahashi et al. Breaching fedmd: Image recovery via paired-logits inversion attack. In *Proc. CVPR Vancouver, BC, Canada*, pages 12198–12207. IEEE, 2023. [2](#)
- [41] Alysa Ziyang Tan et al. Towards personalized federated learning. *IEEE Trans. Neural Networks Learn. Syst.*, 1(1): 1–17, 2022. [1](#)
- [42] Yue Tan et al. Fedproto: Federated prototype learning across heterogeneous clients. In *Proc. AAAI*, pages 8432–8440, virtual, 2022. AAAI Press. [2](#), [6](#), [7](#)
- [43] Laurens van der Maaten and Geoffrey Hinton. Visualizing data using t-sne. *Journal of Machine Learning Research*, 9(86):2579–2605, 2008. [7](#)
- [44] Chuhan Wu et al. Communication-efficient federated learning via knowledge distillation. *Nature Communications*, 13(1):2032, 2022. [2](#), [6](#), [7](#)
- [45] Mang Ye et al. Heterogeneous federated learning: State-of-the-art and research challenges. *CoRR*, abs/2307.10616:1, 2023. [2](#)
- [46] Liping Yi, Gang Wang, Xiaoguang Liu, Zhuan Shi, and Han Yu. Fedgh: Heterogeneous federated learning with generalized global header. In *Proceedings of the 31st ACM International Conference on Multimedia (ACM MM’23)*, page 11, Canada, 2023. ACM. [2](#)
- [47] Fuxun Yu et al. Fed2: Feature-aligned federated learning. In *Proc. KDD*, pages 2066–2074, virtual, 2021. ACM. [2](#)
- [48] Sixing Yu et al. Resource-aware federated learning using knowledge extraction and multi-model fusion. *CoRR*, abs/2208.07978, 2022. [2](#)
- [49] Jie Zhang et al. Parameterized knowledge transfer for personalized federated learning. In *Proc. NeurIPS*, pages 10092–10104, virtual, 2021. OpenReview.net. [2](#)
- [50] Lan Zhang et al. Fedzkt: Zero-shot knowledge transfer towards resource-constrained federated learning with heterogeneous on-device models. In *Proc. ICDCS*, pages 928–938, virtual, 2022. IEEE. [2](#)
- [51] Zhilu Zhang and Mert R. Sabuncu. Generalized cross entropy loss for training deep neural networks with noisy labels. In *Proc. NeurIPS*, pages 8792–8802, Montréal, Canada, 2018. Curran Associates Inc. [4](#)
- [52] Hangyu Zhu et al. Federated learning on non-iid data: A survey. *Neurocomputing*, 465:371–390, 2021. [1](#)
- [53] Zhuangdi Zhu et al. Data-free knowledge distillation for heterogeneous federated learning. In *Proc. ICML*, pages 12878–12889, virtual, 2021. PMLR. [2](#)
- [54] Zhuangdi Zhu et al. Resilient and communication efficient learning for heterogeneous federated systems. In *Proc. ICML*, pages 27504–27526, virtual, 2022. PMLR. [2](#)

pFedES: Model Heterogeneous Personalized Federated Learning with Feature Extractor Sharing

Supplementary Material

8. Proof for Lemma 1

Proof. As formulated in Eq. (5), the local heterogeneous model of an arbitrary client k is updated by

$$\omega_{t+1} = \omega_t - \eta g_{\omega}^t = \omega_t - \eta \nabla((1 - \mu) \cdot \mathcal{L}_{\omega_t} + \mu \cdot \mathcal{L}_{\varphi_t}). \quad (17)$$

Based on Assumption 1 and Eq. (17), we can get

$$\begin{aligned} \mathcal{L}_{tE+1} &\leq \mathcal{L}_{tE+0} + \langle \nabla \mathcal{L}_{tE+0}, (\omega_{tE+1} - \omega_{tE+0}) \rangle + \frac{L_1 \eta^2}{2} \|\omega_{tE+1} - \omega_{tE+0}\|_2^2 \\ &= \mathcal{L}_{tE+0} - \eta \langle \nabla \mathcal{L}_{tE+0}, \nabla((1 - \mu) \cdot \mathcal{L}_{\omega_{tE+0}} + \mu \cdot \mathcal{L}_{\varphi_{tE+0}}) \rangle + \frac{L_1 \eta^2}{2} \|\nabla((1 - \mu) \cdot \mathcal{L}_{\omega_{tE+0}} + \mu \cdot \mathcal{L}_{\varphi_{tE+0}})\|_2^2. \end{aligned} \quad (18)$$

Take the expectations of random variable ξ_{tE+0} on both sides, we have

$$\begin{aligned} \mathbb{E}[\mathcal{L}_{tE+1}] &\leq \mathcal{L}_{tE+0} - \eta \mathbb{E}[\langle \nabla \mathcal{L}_{tE+0}, \nabla((1 - \mu) \cdot \mathcal{L}_{\omega_{tE+0}} + \mu \cdot \mathcal{L}_{\varphi_{tE+0}}) \rangle] + \frac{L_1 \eta^2}{2} \mathbb{E}[\|\nabla((1 - \mu) \cdot \mathcal{L}_{\omega_{tE+0}} + \mu \cdot \mathcal{L}_{\varphi_{tE+0}})\|_2^2] \\ &\stackrel{(a)}{\leq} \mathcal{L}_{tE+0} - \eta \mathbb{E}[\langle \nabla \mathcal{L}_{tE+0}, \nabla((1 - \mu) \cdot \mathcal{L}_{\omega_{tE+0}}) \rangle] + \frac{L_1 \eta^2}{2} \mathbb{E}[\|\nabla((1 - \mu) \cdot \mathcal{L}_{\omega_{tE+0}} + \mu \cdot \mathcal{L}_{\varphi_{tE+0}})\|_2^2] \\ &= \mathcal{L}_{tE+0} - \eta(1 - \mu) \|\nabla \mathcal{L}_{\omega_{tE+0}}\|_2^2 + \frac{L_1 \eta^2}{2} \mathbb{E}[\|\nabla((1 - \mu) \cdot \mathcal{L}_{\omega_{tE+0}} + \mu \cdot \mathcal{L}_{\varphi_{tE+0}})\|_2^2] \\ &\stackrel{(b)}{\leq} \mathcal{L}_{tE+0} - \eta(1 - \mu) \|\nabla \mathcal{L}_{\omega_{tE+0}}\|_2^2 + \frac{L_1 \eta^2}{2} (\text{Var}(\nabla((1 - \mu) \cdot \mathcal{L}_{\omega_{tE+0}} + \mu \cdot \mathcal{L}_{\varphi_{tE+0}})) + \|\nabla((1 - \mu) \cdot \mathcal{L}_{\omega_{tE+0}} + \mu \cdot \mathcal{L}_{\varphi_{tE+0}})\|_2^2) \\ &\stackrel{(c)}{\leq} \mathcal{L}_{tE+0} - \eta(1 - \mu) \|\nabla \mathcal{L}_{\omega_{tE+0}}\|_2^2 + \frac{L_1 \eta^2}{2} ((\sigma^2 + \delta^2) + \|\nabla((1 - \mu) \cdot \mathcal{L}_{\omega_{tE+0}} + \mu \cdot \mathcal{L}_{\varphi_{tE+0}})\|_2^2) \\ &\stackrel{(d)}{\leq} \mathcal{L}_{tE+0} - \eta(1 - \mu) \|\nabla \mathcal{L}_{\omega_{tE+0}}\|_2^2 + \frac{L_1 \eta^2}{2} ((\sigma^2 + \delta^2) + \|\nabla((1 - \mu) \cdot \mathcal{L}_{\omega_{tE+0}})\|_2^2) \\ &= \mathcal{L}_{tE+0} + \left(\frac{L_1 \eta^2 (1 - \mu)^2}{2} - \eta(1 - \mu) \right) \|\nabla \mathcal{L}_{\omega_{tE+0}}\|_2^2 + \frac{L_1 \eta^2 (\sigma^2 + \delta^2)}{2} \\ &\stackrel{(e)}{=} \mathcal{L}_{tE+0} + \left(\frac{L_1 \eta^2 \tilde{\mu}^2}{2} - \eta \tilde{\mu} \right) \|\nabla \mathcal{L}_{\omega_{tE+0}}\|_2^2 + \frac{L_1 \eta^2 (\sigma^2 + \delta^2)}{2}, \end{aligned} \quad (19)$$

where (a) : $\mu \in (0, 0.5]$, $(1 - \mu) \in [0.5, 1)$, $\ell_{\varphi_{tE+0}} \geq 0$, so $\mu \cdot \ell_{\varphi_{tE+0}} \geq 0$. (b) follows from $\text{Var}(x) = \mathbb{E}[x^2] - (\mathbb{E}[x])^2$. (c) follows from Assumption 2. (d) are the same as (a). (e): we denote $1 - \mu = \tilde{\mu}$, $\tilde{\mu} \in [0.5, 1)$.

Take the expectations of the heterogeneous local model ω on both sides across E local iterations, we have

$$\mathbb{E}[\mathcal{L}_{(t+1)E}] \leq \mathcal{L}_{tE+0} + \left(\frac{L_1 \eta^2 \tilde{\mu}^2}{2} - \eta \tilde{\mu} \right) \sum_{e=0}^{E-1} \|\nabla \mathcal{L}_{tE+e}\|_2^2 + \frac{L_1 \eta^2 (\sigma^2 + \delta^2)}{2}. \quad (20)$$

□

9. Proof for Theorem 1

Proof. Eq. (20) can be adjusted further as

$$\sum_{e=0}^{E-1} \|\nabla \mathcal{L}_{tE+e}\|_2^2 \leq \frac{\mathcal{L}_{tE+0} - \mathbb{E}[\mathcal{L}_{(t+1)E}] + \frac{L_1 \eta^2 (\sigma^2 + \delta^2)}{2}}{\eta \tilde{\mu} - \frac{L_1 \eta^2 \tilde{\mu}^2}{2}}. \quad (21)$$

Take the expectations of the heterogeneous local model ω on both sides across T communication rounds, we have

$$\frac{1}{T} \sum_{t=0}^{T-1} \sum_{e=0}^{E-1} \|\nabla \mathcal{L}_{tE+e}\|_2^2 \leq \frac{\frac{1}{T} \sum_{t=0}^{T-1} (\mathcal{L}_{tE+0} - \mathbb{E}[\mathcal{L}_{(t+1)E}]) + \frac{L_1 \eta^2 (\sigma^2 + \delta^2)}{2}}{\eta \tilde{\mu} - \frac{L_1 \eta^2 \tilde{\mu}^2}{2}}. \quad (22)$$

Let $\Delta = \mathcal{L}_{t=0} - \mathcal{L}^* > 0$, then $\sum_{t=0}^{T-1} (\mathcal{L}_{tE+0} - \mathbb{E}[\mathcal{L}_{(t+1)E}]) \leq \Delta$, so we have

$$\frac{1}{T} \sum_{t=0}^{T-1} \sum_{e=0}^{E-1} \|\nabla \mathcal{L}_{tE+e}\|_2^2 \leq \frac{\Delta}{T} + \frac{L_1 \eta^2 (\sigma^2 + \delta^2)}{2 \left(\eta \tilde{\mu} - \frac{L_1 \eta^2 \tilde{\mu}^2}{2} \right)}. \quad (23)$$

If the above equation can converge to a constant ϵ , i.e.,

$$\frac{1}{T} \sum_{t=0}^{T-1} \sum_{e=0}^{E-1} \|\nabla \mathcal{L}_{tE+e}\|_2^2 \leq \frac{\Delta}{T} + \frac{L_1 \eta^2 (\sigma^2 + \delta^2)}{2 \left(\eta \tilde{\mu} - \frac{L_1 \eta^2 \tilde{\mu}^2}{2} \right)} < \epsilon, \quad (24)$$

then

$$T > \frac{2\Delta}{\eta \tilde{\mu} (2 - L_1 \eta \tilde{\mu}) \left(\epsilon - \frac{\eta L_1 (\sigma^2 + \delta^2)}{\tilde{\mu} (2 - L_1 \eta \tilde{\mu})} \right)}. \quad (25)$$

Since $T > 0, \Delta > 0$, so we get

$$\eta \tilde{\mu} (2 - L_1 \eta \tilde{\mu}) \left(\epsilon - \frac{\eta L_1 (\sigma^2 + \delta^2)}{\tilde{\mu} (2 - L_1 \eta \tilde{\mu})} \right) > 0. \quad (26)$$

After solving the above inequality, we can get

$$\eta < \frac{2\epsilon \tilde{\mu}}{L_1 (\sigma^2 + \delta^2 + \tilde{\mu}^2 \epsilon)}. \quad (27)$$

Since $\epsilon, \tilde{\mu}, L_1, \sigma^2, \delta^2 > 0$ are both constants, the learning rate η of the local heterogeneous model has solutions.

Therefore, when the learning rate of the local heterogeneous model satisfies the above condition, an arbitrary client's local heterogeneous local can converge. In addition, on the right side of Eq. (23), except for $\frac{\Delta}{T}$, Δ and other items are both constants, so the non-convex convergence rate $\epsilon \sim \mathcal{O}(\frac{1}{T})$. \square

10. Sensitivity to Hyperparameters

pFedES involves two key hyperparameters: 1) μ , the *weight of the loss* for the combination of the frozen feature extractor and the training local heterogeneous model in step ① of iterative training; 2) E_{fe} , the *training epochs* for the combination of the training feature extractor and the frozen local heterogeneous model in step ② of iterative training. Take the model-heterogeneous experiments with ($N = 100, C = 10\%$) as examples, Fig. 10 displays that the average test accuracy of pFedES varies as $\mu = \{0.1, 0.2, 0.3, 0.4, 0.5\}$ and $E_{fe} = \{5, 10, 15, 20\}$. Model accuracy decreases as μ rises since a larger μ emphasizes more globally generalized knowledge and weakens local personalized knowledge. Model accuracy also drops as E_{fe} increases since a larger E_{fe} may lead the combination of the training feature extractor and the frozen local heterogeneous model to be overfitting.

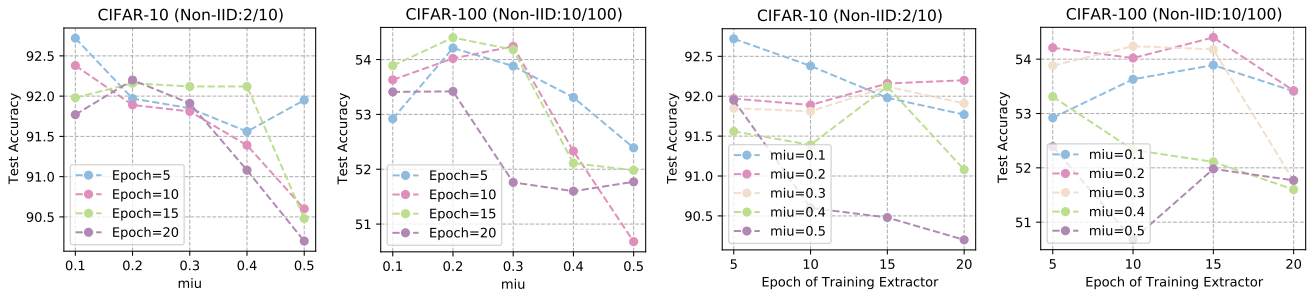


Figure 10. Sensitivity to hyperparameters μ and E_{fe} .